Estimation of the Energy Spectrum in the Knee Region by the KASCADE-Experiment

A.A. Chilingarian[1*], T. Antoni[2], W.D. Apel[2], F. Badea[4], K. Bekk[2], K. Bernlöhr[2], E. Bollmann[2], H. Bozdog[4], I.M. Brancus[4], K. Daumiller[2], P. Doll[2], J. Engler[2], F. Feßler[2], H.J. Gils[2], R. Glasstetter[2], R. Haeusler[2], W. Hafemann[2], A. Haungs[2], D. Heck[2], J.R. Hörandel[2 †], T. Holst[2], K.–H. Kampert[2], J. Kempa[3], H.O. Klages[2], J. Knapp[2 ‡], H.J. Mathes[2], H.J. Mayer[2], J. Milke[2], D. Mühlenberg[2], J. Oehlschläger[2], M. Petcu[4], H. Rebel[2], M. Risse[2], M. Roth[2], G. Schatz[2], F.K. Schmidt[2], T. Thouw[2], H. Ulrich[2], A. Vardanyan[1], B. Vulpescu[4], J.H. Weber[2], J. Wentz[2], T. Wibig[3], T. Wiegert[2], D. Wochele[2], J. Wochele[2], J. Zabierowski[3]

[1] *Yerevan Physics Institute, Cosmic Ray Division, Armenia*[§]

[2] *Institut für Kernphysik and Institut für Experimentelle Kernphysik, Forschungszentrum and Universität Karlsruhe P.O. Box 3640, D–76021 Karlsruhe, Germany*

[3] *Institute for Nuclear Studies and Dept. of Experimental Physics, University of Lodz, PL–90950 Lodz, Poland*

[4] *National Institute of Physics and Nuclear Engineering, RO–7690 Bucharest, Romania*

Abstract

The KASCADE experiment measuring a larger number of EAS observables with an improved sampling of the electron-photon, hadron, and muon components than previous experiments, provides data accurate enough for an event-by-event analysis of the energy dependence of the primary cosmic ray flux in the energy range of $10^{14} - 10^{16}$ eV. Multivariate statistical analysis approaches enable to estimate the primary cosmic ray flux and the elemental composition. The major feature in the observed PeV energy region, the so called *knee* is reproduced, spectral indices and the knee energy are determined.

1 Introduction:

The knowledge of the energy spectra of primary cosmic rays in the knee region is of great importance for testing alternative hypotheses of the cosmic ray (CR) origin, acceleration, and propagation. The manifold interpretations of CR experiments have their causal connection in the inadequate knowledge about the characteristics of hadronic interactions above accelerator energies. Moreover uncertainties in the CR composition, caused by strong fluctuations of the shower parameters give rise to this ambiguities. The different detector types of the KASCADE experiment (Klages, 1997) measure simultaneously the three charged shower components. This allows not only to take the whole valuable information of EAS showers into account, but to make cross checks in estimating the energy and mass of individual events by different observables. Systematic effects by using various observables e.g. for energy estimation can be studied.

2 EAS Reconstruction:

2.1 The detector setup: The basic concept of the KASCADE experiment is to measure a large number of observables for each individual event with good accuracy and high degree of sampling. For this reason 252 detector stations forming a detector array of $200 \times 200\mathrm{m}^2$ containing liquid scintillation detectors for detecting the electromagnetic component on the top of a lead/iron absorber plate as well as plastic scintillators below the shielding. A detector coverage of more than 1% for the electromagnetic and about 2% for the muonic component EAS is achieved. In combination with a precise measurement of the hadrons using a large iron sampling calorimeter the shower core can be investigated in great detail. So the main part of the central detector

[*] corresponding author: e-mail: chili@ik3.fzk.de

[†] now at: University of Chicago, Enrico Fermi Institute, Chicago, IL 60637

[‡] now at: University of Leeds, Leeds LS2 9JT, U.K.

[§] The work has been partly supported by a research grant (No.94964) of the Armenian Government and by the ISTC project A116.

system is a large hadron calorimeter. It consists of an $20 \times 16\ \mathrm{m}^2$ iron stack with eight horizontal gaps. 10,000 ionisation chambers are used in six gaps and below the iron stack for the measurement of hadronic energy in a total of 40,000 electronic channels. The third gap is equipped with 456 scintillation detectors for triggering and timing purposes. Below the iron stack two layers of multiwire proportional chambers (MWPCs) are mounted for the measurement of muon tracks and studies of structures in the muon lateral distribution in EAS cores.

2.2 Relevant Observables: The presented detailed analysis of EAS benefits from the simultaneous measurement of a large number of quantities for each individual event. This enables multidimensional analyses for the reconstruction of the energy and the mass of the primary. Specific EAS parameters measurable by the experiment KASCADE are used, like the number of electrons N_e, the truncated number of muons N_μ^{tr} (Glasstetter, 1997; Weber, 1997), the number of reconstructed hadrons N_h^{100GeV} with an energy larger than 100 GeV, the sum of the energy of this hadrons $\sum E_h$, the energy of the mostenergetic hadron $\max E_h$ (Hörandel, 1997) and the number of muons $N_\mu^\star$ with an energy threshold of $E_\mu \geq 2$ GeV measured below the central calorimeter by the MWPCs (Haungs, 1996).

Two sets of data are used. "Selection I" uses the information from the array of field stations on electrons and muons. It permits to analyse the data with good statistical accuracy but has no information from the central detector. "Selection II" uses in addition many observables measured in the central detector but has the disadvantage of a reduced data sample (Roth, 1999).

Therefore 720,000 events with an energy larger than $E \approx 5 \cdot 10^{14}\,\mathrm{eV}$ and a maximal core distance to the centre of the field array of 91 m are selected (set "selection I"). Approximately 8000 high-energetic ($E > 10^{15}\,\mathrm{eV}$), central showers are collected by cuts of N_μ^{tr} ($> 10^{3.6}$), the core location ($R_{core} < 5\,\mathrm{m}$ from the centre of the central detector system), at least one hadron with an energy above 100 GeV and 10 muons in the MWPCs (set "selection II").

2.3 Simulations: Simulations have been performed with the models VENUS and QGSJet in the energy range $10^{14} - 3.16 \cdot 10^{16}$ eV using the CORSIKA code (Heck, 1998).

For each primary (p, He, O, Si, and Fe) approximately 2000 EAS events have been simulated, distributed in the energy range with an decreasing particle flux. The core of the EAS lies within a 5 m radius away from the centre of the central detector. The response of all detector components is taken into account in great detail using the GEANT code. Afterwards the simulated events are treated like measured ones, therefore measured and simulated data are stored and furthermore reconstructed with the same procedures.

3 Energy Estimation:

The techniques presented by Chilingarian (Chilingarian, 1998) on the basis of nonparametric multivariate methods (neural networks, Bayesian decision making) are developed and applied to infer the energy and/or the mass of primary particles on an event-by-event analysis.

The best summary of accumulated knowledge in simulation trials are the nonparametric multidimensional

	QGSJet	VENUS
γ_1	$2.72 \pm 0.003 \pm 0.03$	$2.87 \pm 0.003 \pm 0.04$
γ_2	$3.22 \pm 0.05 \pm 0.06$	$3.25 \pm 0.04 \pm 0.06$
E_{knee} [10^6 GeV]	$6.39 \pm 0.14 \pm 0.7$	$6.22 \pm 0.27 \pm 0.8$
ϵ	$14.10 \pm 5.58 \pm 5.$	$11.61 \pm 4.04 \pm 6.$
χ^2/dof	3.90	3.68

Table 1: Spectral indices and different other parameters as a result of the fitting procedure (including statistical and systematical errors).

probability density functions as well as a set of weights of "trained" neural networks. Due to the stochastic nature of the cascade development in the atmosphere it can't be expected that analytic probability distributions will describe any measurable EAS parameter. Moreover, very long (usually unregular) tails of the parameter distributions require considerable large amount of simulations to map all possible misclassifications and errors.

The Feed-Forward Neural Network (FFNN) provides the mapping of a complicated input signal to the regressand value (energy) in the estimation case (and to the class assignments in the classification case) (Chilingarian, 1994, 1997). The network training is performed by minimising a special quality function Q. The figure of merit to be minimised is simply the discrepancy of apparent and target outputs over all training samples M_k of all primaries $k \in \{p, O, Fe\}$.

The network has typically a $2 \times 5 \times 3 \times 1$ topology using N_e, N_μ^{tr} as input and the energy as output parameters.

The fitting function to the energy response function (output) is

$$f(E) = c \cdot E^{-\gamma_1} \left(1 + \left(\frac{E}{E_{knee}}\right)^{\epsilon}\right)^{\frac{\gamma_1 - \gamma_2}{\epsilon}}.$$

Table 1 displays the results of the fitting procedure. The parameter ϵ describes the curvature of the knee feature. A small one (e.g. $\epsilon = 1$) gives a sharp and a large one (e.g. $\epsilon = 40$) a smooth knee.

The all-particle energy spectrum resulting from different networks shows strong model dependence ($\gamma_{QGSJet} = 2.72$ and $\gamma_{VENUS} = 2.87$; see figure 1). The slope difference 0.16 between the models below the knee is even larger than the methodical errors of 0.04.

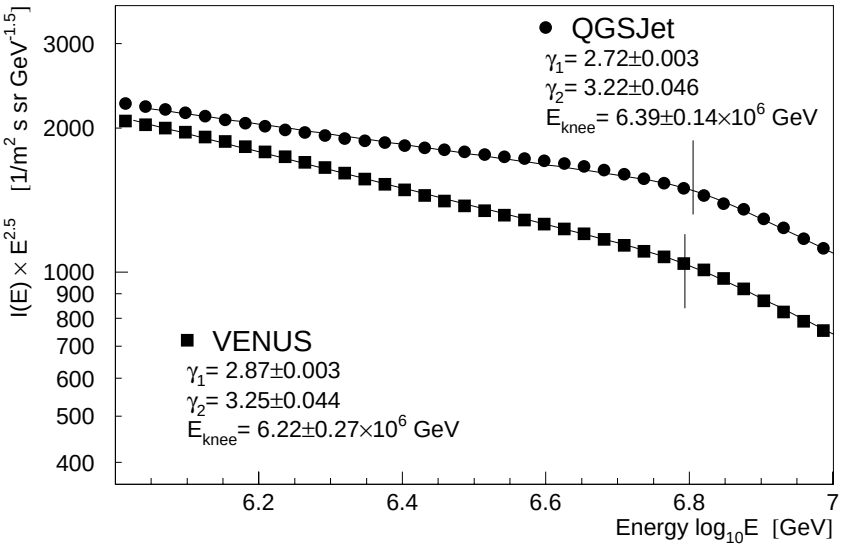

Figure 1: All particle energy spectrum of "selection I" data (see text for explanation) as a result of a neural net analysis (QGSJet and VENUS data trained networks were used).

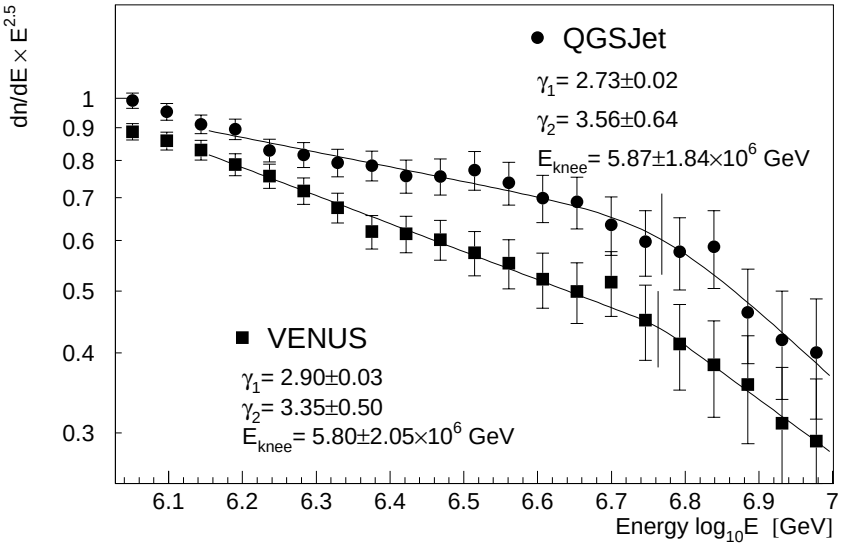

Figure 2: All-particle energy spectrum of "selection II" data with ordinate units (see text for explanation) as a result of a neural net analysis (QGSJet and VENUS data trained networks were used).

To proof the possibility of selecting different data sets without introducing systematic errors, the same trained network (N_e, N_μ^{tr}, s) was applied to estimate the energy of the "selection II" events. The resulting energy spectrum is given in figure 2. Within the statistical errors

the spectral indices (QGSJet and VENUS) below the knee are the same as in figure 1. There aren't enough measured events above the knee to reconstruct a reasonable index with small statistical errors. These events provide nevertheless the opportunity to estimate the spectral index below the knee by using different sets of observables in neural net analyses. The good agreement of the resulting indices is shown in case of QGSJet trained networks in table 2.

	Spectral Index	Observables
	$2.72 \pm 0.003 \pm 0.02$	selection I $N_e,\ N_\mu^{tr}, s$
	$2.73 \pm 0.03 \pm 0.05$	selection II $N_e,\ N_\mu^{tr}, s$ *
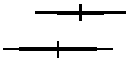	$2.70 \pm 0.05 \pm 0.05$	selection II $N_\mu^{tr},\ N_\mu^{\star}$ *
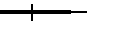	$2.74 \pm 0.05 \pm 0.05$	selection II $N_\mu^{tr},\ N_h^{E>100\,\mathrm{GeV}}$ *
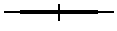	$2.74 \pm 0.05 \pm 0.05$	selection II $N_\mu^{\star},\ N_h^{E>100\,\mathrm{GeV}}$ *
	$2.71 \pm 0.04 \pm 0.05$	selection II $N_\mu^{\star},\ \sum E_h$ *
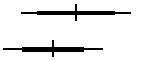	$2.75 \pm 0.05 \pm 0.09$	selection II $N_\mu^{\star},\ \max E_h$ *
	2.73 ± 0.05	all (*) averaged

Table 2: Spectral index γ_1 below the knee (QGSJet simulations) as a result of the neural net analysis. (The systematic errors are estimated by different types of network topologies.)

The results of the presented analyses on the energy dependence of the all-particle spectrum have preliminary character due to the insufficient amount of simulated events and also the lag of central detected showers to determine spectral indices above the knee. Nevertheless the major feature of the observed energy region (the abrupt change of the spectrum) is reproduced. Taking different sets of observables the resulting spectral indices remain the same within the statistical errors. The results show the necessity of investigating the model dependence in detail in order to overcome artifical features of specific models and to get reliable information for understanding origin, acceleration, and propagation of cosmic rays.

References

Chilingarian, A. et al., Proc. 16th ECRS (Madrid, 1998), 571
Chilingarian, A.A. 1994, *Neurocomputing* 6, 497
Chilingarian, A.A. et al. 1997, *Nuclear. Phys. B (Proc. Suppl.)* 52B, 237
Glasstetter, R. et al., Proc. 25th ICRC (Durban, 1997) Vol 6, 157
Haungs, A. et al. 1996, *Nucl. Instr. Meth.* A372, 515
Heck, D. et al. 1998, FZKA-Report 6019, Forschungszentrum Karlsruhe, Germany
Hörandel, J.R. et al., Proc. 25th ICRC (Durban, 1997) Vol 6, 93
Klages, H.O. et al. 1997, *Nucl. Phys. B (Proc. Suppl.)*, 52B, 92
Roth, M. 1999, FZKA-Report 6262, Forschungszentrum Karlsruhe, Germany
Weber, J.H. et al., Proc. 25th ICRC (Durban, 1997) Vol 6, 153